



Is There a Disk of Satellites around the Milky Way?

Moupiya Maji^{1,2}, Qirong Zhu^{1,2,3}, Federico Marinacci⁴, and Yuexing Li^{1,2}

¹ Department of Astronomy & Astrophysics, The Pennsylvania State University, University Park, PA 16802, USA; moupiya@psu.edu

² Institute for Gravitation and the Cosmos, The Pennsylvania State University, University Park, PA 16802, USA

³ Harvard-Smithsonian Center for Astrophysics, Harvard University, 60 Garden Street, Cambridge, MA 02138, USA

⁴ Department of Physics, Kavli Institute for Astrophysics and Space Research, Massachusetts Institute of Technology, Cambridge, MA 02139, USA

Received 2017 January 26; revised 2017 May 5; accepted 2017 May 12; published 2017 July 3

Abstract

The “disk of satellites” (DoS) around the Milky Way is a highly debated topic with conflicting interpretations of observations and their theoretical models. We perform a comprehensive analysis of all of the dwarfs detected in the Milky Way and find that the DoS structure depends strongly on the plane identification method and the sample size. In particular, we demonstrate that a small sample size can artificially produce a highly anisotropic spatial distribution and a strong clustering of the angular momentum of the satellites. Moreover, we calculate the evolution of the 11 classical satellites with proper motion measurements and find that the thin DoS in which they currently reside is transient. Furthermore, we analyze two cosmological simulations using the same initial conditions of a Milky-Way-sized galaxy, an N -body run with dark matter only, and a hydrodynamic one with both baryonic and dark matter, and find that the hydrodynamic simulation produces a more anisotropic distribution of satellites than the N -body one. Our results suggest that an anisotropic distribution of satellites in galaxies can originate from baryonic processes in the hierarchical structure formation model, but the claimed highly flattened, coherently rotating DoS of the Milky Way may be biased by the small-number selection effect. These findings may help resolve the contradictory claims of DoS in galaxies and the discrepancy among numerical simulations.

Key words: galaxies: dwarf – galaxy: evolution – hydrodynamics – methods: numerical

1. Introduction

Four decades ago, it was first reported that five bright satellite galaxies of the Milky Way (MW) align in a plane inclined to the Galactic stellar disk (Lynden-Bell 1976), a phenomenon later dubbed the “disk of satellites” (DoS) (Kroupa et al. 2005) that included 11 bright MW dwarfs. Recently, it was claimed that eight of these satellites co-rotate in the DoS (Metz et al. 2008; Pawlowski & Kroupa 2013). Numerical simulations with the standard Λ CDM model have been largely unsuccessful in reproducing such a spatially thin, kinematically coherent structure, which has been strongly criticized as a failure of the standard Λ CDM cosmology (Kroupa et al. 2005; Pawlowski et al. 2015a).

To date, more than three dozen dwarf galaxies have been detected around the MW (McConnachie 2012; Koposov et al. 2015), and it was suggested that all of the satellites lie in the original DoS formed by the 11 classical satellites (Pawlowski et al. 2015b). More intriguingly, it was recently reported that about half of the satellites in Andromeda (15 out of 27) form a DoS around the host (McConnachie et al. 2009; Conn et al. 2013; Pawlowski & Kroupa 2013), and that 13 of the 15 co-planar satellites co-rotate based on line-of-sight velocities (Ibata et al. 2013). Outside of the Local Group, one study (Ibata et al. 2014) found 22 galaxies in the Sloan Digital Sky Survey (SDSS) catalog which have diametrically opposed satellite pairs with anti-correlated velocities, and the authors suggested that co-planar and co-rotating disks of satellites are common in the Universe.

The origin of the DoS, however, has remained an unsolved mystery. On the one hand, many advanced Λ CDM simulations have failed to produce such thin, co-rotating disks of satellites in galaxies. While some sophisticated simulations have managed to produce an anisotropic distribution of satellites

(Pawlowski et al. 2015a; Buck et al. 2016; Papastergis & Shankar 2016; Sawala et al. 2016; Zhu et al. 2016), no consensus of coherent motion was found in the DoS (Bahl & Baumgardt 2014; Cautun et al. 2015a; Buck et al. 2016; Sawala et al. 2016).

On the other hand, the interpretation of the DoS from observations has been called into question. Buck et al. (2016) demonstrated that line-of-sight velocities are not representative of the full 3D velocity of a galaxy and they cannot be used to derive coherent motion in Andromeda satellites. Furthermore, recent investigations of the SDSS galaxies by Cautun et al. (2015b) and Phillips et al. (2015) found that the excess of pairs of anti-correlated galaxies is very sensitive to sample selection and is consistent with the random noise corresponding to an under-sampling of the data.

In order to resolve the controversies surrounding the DoS, we reanalyze the observed satellites of the MW and compare them with advanced simulations. We focus on the following important issues: (1) effects of the plane identification method and sample size on the DoS properties, (2) the stability of the planar structure, and (3) effects of baryons on the distribution and evolution of satellites.

The paper is organized as follows. In Section 2 we introduce the methods used in this study, including the techniques to identify the planar structure, the model to project future evolution of the current satellites, and the cosmological simulations with and without baryons. We present our results in Section 3, namely the structural and kinematic properties of the observed satellites using different plane identification methods and sample sizes in Section 3.1, the dynamical evolution of the observed 11 classical satellites in Section 3.2, and the DoS structure and its evolution from two cosmological simulations in Section 3.3. We summarize our findings and their implications in Section 4.

2. Methods

We use two types of techniques to analyze the present distribution of the positions of the observed satellites around the MW: the principal component analysis (PCA) and the tensor of inertia (TOI).

For our specific case of 3D positional data, PCA can be thought of as fitting an ellipsoid to the data, where the ratio of minor and major axis (c/a) indicates the anisotropy of the dwarf distribution. If the distribution of the dwarfs is perfectly planar, then $c/a \rightarrow 0$. In the TOI method, which is often used in literature (Allgood et al. 2006), we calculate the moment of inertia matrix of the satellites and diagonalize it. The eigenvalues of this matrix gives the three axes (a, b, c) of the fitted ellipsoid to the dwarf distribution. It has been argued that distant dwarfs in this distribution have a greater chance of being outliers, hence they should carry less weight in the TOI calculations. Here we consider three different weights for satellite distances, namely 1 , $1/r$ and $1/r^2$, respectively, as used by different groups in literature (Cautun et al. 2015b; Pawlowski et al. 2015a; Sawala et al. 2016). We discuss these methods in more detail in a companion paper (M. Maji et al. 2017, in preparation).

Moreover, in order to investigate the stability of the DoS, we employ the galaxy dynamics software Galpy⁵ (Bovy 2015) to predict the future position and velocity of the observed 11 classical satellites. We use a realistic MW potential with three components: a power-law density profile (cut off at 1.9 kpc) for the central bulge, a stellar disk represented by a combination of three Miyamoto–Nagai potentials (MN3 model) with varying disk mass and radial scalelength (Smith et al. 2015), and a Navarro–Frenk–White (Navarro et al. 1996) density profile for the dark matter halo. We take the initial position and velocities in galactic coordinates from Pawlowski & Kroupa (2013) and convert them into galactocentric cartesian coordinates (Johnson & Soderblom 1987).

Finally, in order to understand the origin of the DoS, we compare two cosmological simulations of a MW-sized galaxy, one with both baryons and dark matter (hereafter referred to as “Hydro simulation”; Marinacci et al. 2014) and the other with dark matter only (hereafter referred to as “DMO simulation”; Zhu et al. 2016). The Hydro simulation includes a list of important baryonic physics, such as a two-phase ISM, star formation, metal cooling, and feedback from stars and active galactic nuclei (AGNs). We refer the reader to Marinacci et al. (2014) for more details on this simulation. The dwarf galaxies (subhalos) in the simulations are identified using the Amiga Halo Finder (Knollmann & Knebe 2009), a density-based group finder algorithm.

3. Results

3.1. DoS Properties with Different Methods and Sample Sizes

3.1.1. Structural Properties

A comparison of the DoS structure using different plane identification methods (PCA and TOI) and different sample sizes is illustrated in Figure 1. The sample of 39 currently confirmed dwarfs of the MW (McConnachie 2012; Koposov et al. 2015) includes the 11 classical satellites (Kroupa et al. 2005) and the 27 most massive nearby ones in the previous

analysis (Pawlowski & Kroupa 2013). Clearly, when the satellite number increases from the original 11 to the full sample of 39, the “isotropy” of the DoS (represented by the ratio between semiminor and semimajor axes of the principal components, c/a) increases from $c/a \sim 0.2$ to ~ 0.26 using the PCA and unweighted TOI methods, and the “thickness” of the DoS (represented by the root-mean-square height of the fitted plane) increases rapidly from ~ 20 to ~ 30 kpc. For a weighted TOI with $1/r^2$ typically used in the analysis of cosmological simulations (Sawala et al. 2016), the DoS becomes more isotropic and thicker. This figure demonstrates that the DoS structure is subjected to selection effects, which explains the different claims reported in the literature using different methods and sample sizes (Sawala et al. 2016; Pawlowski et al. 2015b).

In order to test the effect of sample size on the anisotropy measurements in more detail, we sample an isotropic distribution (input c/a and $b/a = 1$) with 10^4 objects. We repeatedly draw random samples of a given size from the sphere and calculate c/a and b/a ratios of the sample using the unweighted TOI method. The variation of these anisotropy ratios with the sample size is shown in Figure 2. For a large sample size N , the output ratios do point to the true results of both ratios being 1. On the other hand, for a small sample size (e.g., $N \sim 10$), it does not adequately sample the sphere, resulting in very biased estimates (for $N = 10$, median $c/a = 0.58$, $b/a = 0.8$). We discuss this effect in more detail in a companion paper (M. Maji et al. 2017, in preparation), where we place 11 satellites at their observed distances, vary the input c/a from 0.4 to 1.0, and perform a Monte Carlo simulation with 10^5 realizations. We find that for all input c/a values, the output c/a is consistently biased toward a lower value. With an input $c/a \sim 0.4$, there is a 20% chance that the system has $c/a \lesssim 0.18$. We also find that the weighted TOI method ($1/r^2$) consistently yields a better result (closer to true value) compared to the unweighted method. This analysis indicates that the system appears to be more anisotropic when the sample size is very small because a small sample size systematically yields a lower c/a ratio than the true underlying anisotropy of the system.

3.1.2. Kinematic Properties

In a recent study by Pawlowski & Kroupa (2013), it was suggested that 7 to 9 out of the 11 classical MW satellites are co-rotating because the angles between their angular momenta and the DoS normal of the 11 satellites fall within 45° . We use the same criterion for co-rotation in this study and show the angular momentum distribution of the satellites in Figure 3. As shown in the left panel of the Figure 8, satellites appear in the co-rotation region (similar to the result of Pawlowski & Kroupa 2013), but given the large error bars of Sextans and Carina, only six (LMC, SMC, Draco, UMi, Fornax, and LeoII) can be robustly considered as co-rotating. However, this sample size is very small and apparent clustering can often be found in random distributions. This effect, known as the clustering illusion (Clarke 1946), can lead to misinterpretation of the data, as we demonstrate below.

In order to understand the significance of the co-rotation and the effect of sample size, we perform a “clustering” test. Our null hypothesis is that there is no coherent motion on the DoS plane; i.e., there is no clustering of the angular momentum on the sphere. We use Monte Carlo simulations to numerically test

⁵ <http://galpy.readthedocs.io/en/latest/>

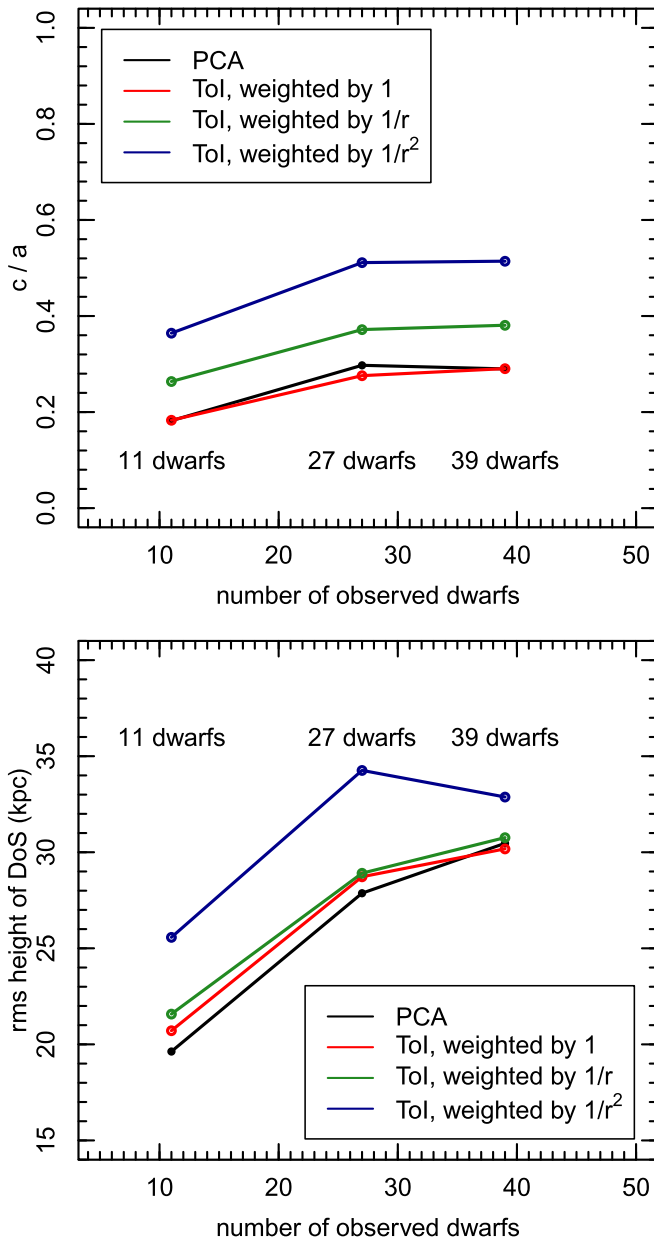


Figure 1. Comparison of the DoS structure using different sample sizes and the plane-fitting method: “isotropy” (top) as indicated by the ratio between semiminor and semimajor axes, c/a ($c/a = 0$ means completely anisotropic planar distribution); and “thickness” (bottom) as indicated by the root-mean-square height of the fitted plane. The plane-fitting methods include PCA and TOI with different weight function. The complete sample includes 39 confirmed satellites of the MW (McConnachie 2012; Koposov et al. 2015).

the apparent clustering seen in the observed satellite angular momenta. We draw N random data points from a uniform distribution on a sphere and search for clustering for each draw within a given apex angle. This experiment is repeated for 10^4 trials. First, we carry out this experiment with a fixed number $N = 11$; i.e., the number of classical MW satellites. It is found that the median number of clustered points within 45° is four, and the chance of finding five or six clustered points within 45° , similar to the clustering for observed satellites, is $\sim 19\%$ for five and $\sim 6\%$ for six points, respectively. Next, we repeat the simulation with a varying number of points. To quantify the effect of sample size, we define a bias parameter as the ratio between the observed number of clustered points and an

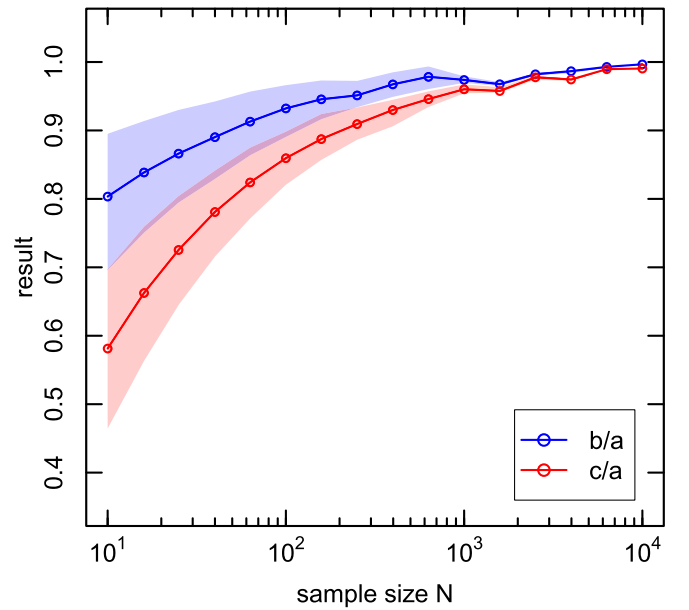


Figure 2. Effects of sample size on the anisotropy measurement of a system. The red and blue lines represent the c/a and b/a ratio of the sample, respectively, and the shaded regions indicate the 1σ error bar of the measurements.

expected number proportional to the solid angle (S) of the cone ($S/4\pi \times N$). The resulting distribution of clustering from these experiments are shown in Figure 3.

This figure demonstrates that for a smaller sample size, the clustering bias is significantly higher at given small angles. A strong clustering factor (2.5–3.5) at $N < 20$ and angle $< 45^\circ$ can be found due to the intrinsic fluctuations of random points alone. This test shows that, even though the intrinsic distribution is uniform, the points can appear highly clustered for a small sample size. Therefore, we caution that the evidence of coherent rotation in the 11 observed satellites may not be conclusively different from that of a random data sample.

3.2. Dynamical Evolution of Satellites

Recently, Lipnicky & Chakrabarti (2017) studied the dynamics history of the 11 classical satellites and suggested that the DoS would lose its significance in less than 1 Gyr in the past. In order to investigate the future evolution of the DoS, we use the galactic dynamics software Galpy (Bovy 2015) to predict the future trajectories of the 11 classical satellites.

Figure 4 shows the future positions of the 11 satellites using a realistic MW potential with three components: a dark matter halo with the NFW density profile (Navarro et al. 1996), a central bulge with a power-law density profile cut off at 1.9 kpc, and a stellar disk with the MN3 potential (Smith et al. 2015). Note that the points only represent the final positions at these times, not the detailed orbits of the satellites, and that nearby satellites such as Sagittarius may complete more than one orbit in 1 Gyr, while distant ones such as LeoII may move only a fraction of their orbits. To estimate the error bars in the positions, we model the present velocities as a normal distribution taking as a standard deviation their present-day uncertainties. We take 1000 random samples from this velocity distribution, calculate their future trajectories, and take the 16th and 84th percentile value (which approximate the 1σ confidence interval) of these future position distribution as

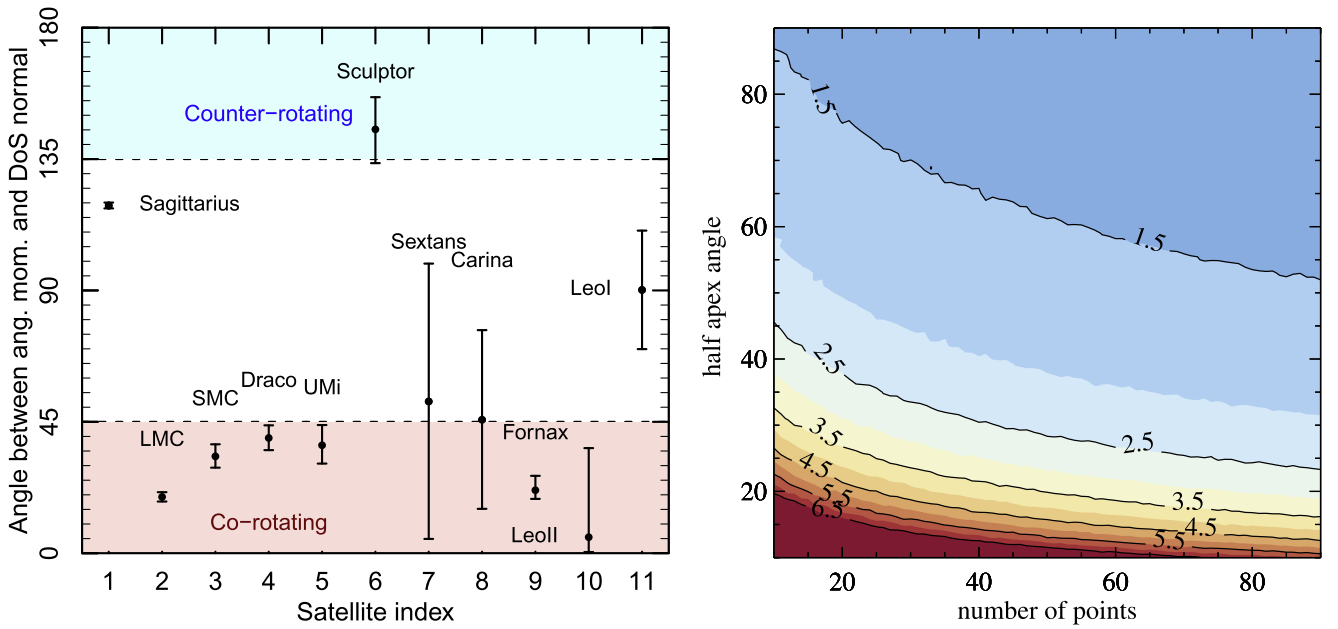


Figure 3. Left panel: distribution of the angle between the satellite angular momentum and the DoS normal, with their respective error bars resulting from the uncertainties in velocity measurements. Satellites can be considered as co-rotating on the DoS if this angle is within 45° (pink region) and counter-rotating if they are within 135° – 180° (green region). Right panel: half-apex angle of the cone vs. the number of points found in them. We draw random data points from a isotropic point distribution in a sphere and search for clustering within different half-apex angle cones in each of the 10^4 trials. The numbers on the contours represent bias parameters. For 11 satellites in a uniform distribution, there is a 6% chance that six of them are clustered within 45° .

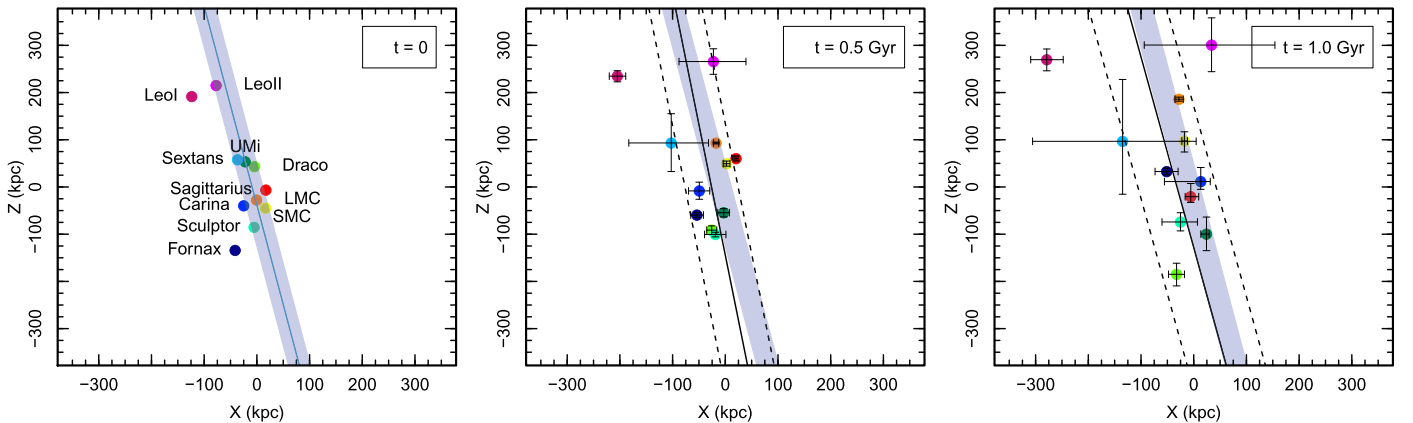


Figure 4. Positions of 11 classical satellites in galactocentric coordinates at the present (left), 0.5 Gyr (middle), and 1 Gyr from now (right), respectively. The solid lines in each panel represent the fitted DoS at that time and the dashed lines represent the rms height of the plane. The blue shaded region in each panel depicts the present-day DoS.

our lower and upper error bars. Some of these satellites have large proper motion errors that propagate a significant uncertainty in far-future positions, so predictions beyond 1 Gyr are not reliable (Lipnicky & Chakrabarti 2017).

From this figure, we find that the 11 satellites are moving away from the present DoS at future times. The new fitted DoS is thicker with $c/a \sim 0.36$ (height 45 kpc) at $t = 0.5$ Gyr and $c/a \sim 0.42$ (height 64 kpc) at $t = 1$ Gyr, compared to the thin DoS (c/a 0.18, height 19.6 kpc) at the present time. We have also explored two different MW potentials, by replacing the stellar disk with a one-component Miyamoto–Nagai potential (Bovy 2015; MW2014 model), and a NFW dark-matter-halo-only potential, but the resulting positions (not shown to avoid overcrowding) are very similar to those from Figure 4. These calculations show that, for these idealized potentials, the MW satellites tend to move away from the present DoS, increasing

its thickness and suggesting that the current thin DoS may be a transient structure.

3.3. Evolution of DoS Isotropy in Simulations

In order to understand the nature and the origin of the DoS, we analyze the satellites from two cosmological simulations of a MW-sized galaxy, the Hydro simulation with comprehensive baryonic physics including star formation and feedback processes (Marinacci et al. 2014), and the DMO simulation which is a pure N -body run (Zhu et al. 2016). We find that baryons can significantly affect the abundance and spatial distribution of satellites (see also Zhu et al. 2016). For example, within 1 Mpc, only 106 luminous subhalos with star formation are found in the Hydro simulation and they are distributed anisotropically, in sharp contrast to the ~ 21220 subhalos which show isotropic distribution in the DMO simulation.

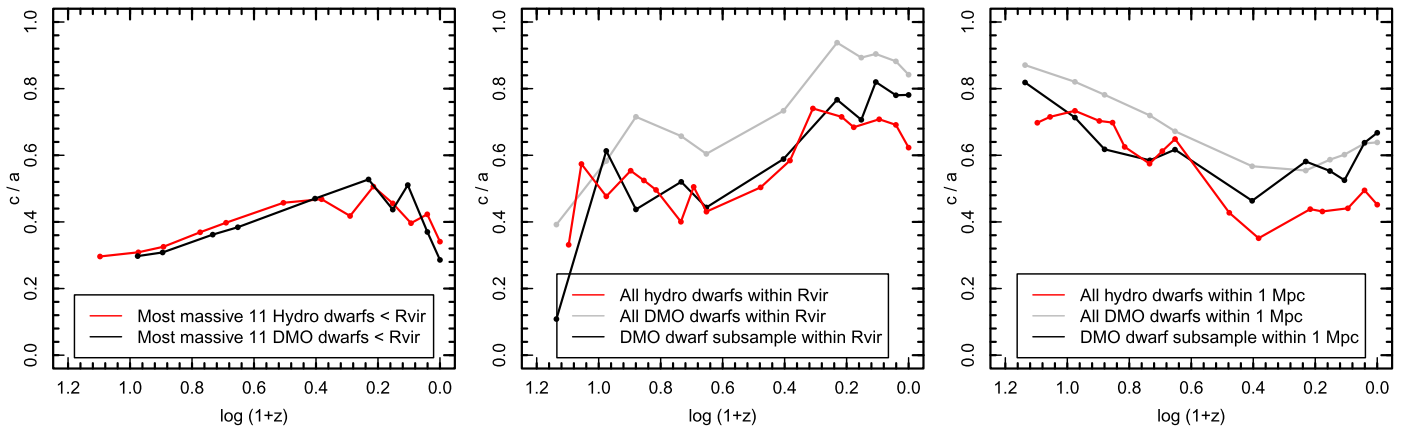


Figure 5. Comparison of the spatial distribution of satellites, as indicated by the “isotropy” c/a , at different redshift between the Hydro and DMO cosmological simulations. We consider three satellite samples: the 11 most massive dwarfs within the virial radius (left panel), dwarfs within the virial radius (R_{vir}) of the central galaxy (middle panel), and dwarfs within 1 Mpc from the central galaxy (right panel). Note that in this figure, “Hydro dwarfs” (in red in all three panels) refer to star-forming dwarfs from the Hydro simulation within a given distance at different redshift (for convenient comparison, let N_{star} be the number of these baryonic dwarfs at a given z), “DMO dwarf subsample” (in black in the middle and right panels) refers to a selective DMO dwarf sample that has the same number as that of the Hydro dwarfs (the N_{star} most massive ones from the DMO simulation at the same redshift and within the same distance considered), and “All DMO dwarfs” (in gray in the middle and right panels) refers to all dwarfs formed from the DMO simulation at the given redshift. All distances are in comoving coordinates.

Figure 5 shows the isotropy ratio c/a of both simulations as a function of redshift for three samples: the 11 most massive dwarfs within the virial radius (which have a similar mass range as the observed 11 classical satellites of the MW), dwarfs within the virial radius of the central galaxy, and dwarfs within 1 Mpc from the galaxy. These groups show three distinct trends in the evolution of c/a . When we select only the 11 most massive halos within the virial radius, the two simulations show similar highly anisotropic distribution throughout time, and at $z = 0$ the c/a ratio is close to the observed value (~ 0.2). For dwarfs within R_{vir} , the c/a ratio generally increases as redshift approaches $z = 0$ for all three samples; i.e., the Hydro dwarfs, all of the DMO dwarfs, and the DMO dwarf subsample (massive DMO dwarfs with the same sample size as the Hydro counterpart). This is mainly due to the rising abundance of dwarfs within the virial radius and phase mixing (Henriksen & Widrow 1997). The satellite infall near the center can be chaotic, and even if some satellites are accreted as a group from similar directions, as they move through the galactic potential the neighboring satellites in phase-space can become out of phase with time, resulting in a smooth phase-space distribution of satellites. This phase mixing is more effective for satellites closer to the center (Helmi et al. 2003), which may explain the increased c/a inside R_{vir} .

On a galactic scale of 1 Mpc from the central galaxy, we find a remarkable difference between the Hydro and DMO simulations. At high redshift ($z \sim 10$) the satellite distributions are almost isotropic, but over time the c/a ratio of both simulations declines, although the decrease is much more significant in the Hydro simulation ($c/a \sim 0.4$ at $z = 0$) compared to the DMO one ($c/a \sim 0.64$ at $z = 0$), even with the same sample size.

On a cosmic scale (> 1 Mpc), we find that both ratios (b/a and c/a) continue to decrease, which suggest that the anisotropic dwarf distribution may be part of the large-scale filamentary structure. We discuss this in more detail in a companion paper (M. Maji et al. 2017, in preparation). Our results suggest that on Mpc scales, the distribution of dwarfs around a central galaxy is anisotropic as part of the large-scale filamentary structure. It has been suggested by many detailed DMO simulations that anisotropic satellite distribution can

result from filamentary accretion of the satellites around the host galaxy, and that the infall history can impact the final orientation of the satellites in the position–velocity space (Aubert et al. 2004; Libeskind et al. 2005; Lovell et al. 2011; Libeskind et al. 2014; Tempel et al. 2014; Buck et al. 2016).

There are two factors responsible for the different satellite distributions between the Hydro and DMO simulations: the difference in the satellite abundance and the effects of baryonic processes. Overall, the satellite abundance in the DMO simulation is much higher than that in the Hydro simulation, which in turn results in a more isotropic distribution, which is evident in Figure 5 (middle panel). Furthermore, in the Hydro simulation the dwarfs are subjected to additional baryonic processes; e.g., adiabatic contraction, tidal disruption, and reionization (Zhu et al. 2016) that can significantly change the abundance, star formation activity, infall time, and trajectory of the satellites. For very massive subhalos the effects are mild and the most massive halos in both simulations are essentially the same, resulting in very similar c/a evolution for the 11 massive satellites. However, for intermediate-mass halos the tidal effects impact the dynamics of the halos and, even in similar mass range, halos in the DMO and Hydro simulations have different properties. Hence, in spite of having the same sample size, the halos within 1 Mpc show a significantly different distribution for simulations with and without baryons. Similar results have also been suggested by recent studies (e.g., Zolotov et al. 2012; Ahmed et al. 2016; Sawala et al. 2016; Zhu et al. 2016). Therefore, the inclusion of baryonic impacts may solve the discrepancy in the DoS anisotropy from previous simulations (Pawlowski et al. 2015a; Sawala et al. 2016).

4. Conclusions

In summary, we have performed a comprehensive reanalysis of the observed satellites of the MW using different plane identification methods and sample sizes. We have carried out Monte Carlo simulations to investigate the effects of sample size on the DoS properties, calculated the future evolution of the 11 classical satellites in order to test the stability of the current DoS, and compared two cosmological simulations in order to understand the evolution of satellites and effects of

baryons on the DoS properties. We find that the measured DoS properties strongly depend on the plane identification method and the sample size, and that a small sample size may artificially show high anisotropy and strong clustering. Furthermore, we find that the DoS structure may be transient, and that baryonic processes play an important role in determining the distribution of satellites. We conclude that the evidence for an ultra-thin, coherently rotating DoS of the MW is not conclusive. Our findings suggest that the spatial distribution and kinematic properties of satellites may be determined by the assembly history and dynamical evolution of each individual galaxy system, rather than being a universal DoS phenomenon.

Y.L. acknowledges support from NSF grants AST-0965694, AST-1009867, AST-1412719, and MRI-1626251. We thank the anonymous referee, Dr. Marcel Pawlowski, and Dr. Yohan Dubois for thoughtful comments that helped improve our manuscript. We thank Dr. Jo Bovy for helping us with the Galpy software. We acknowledge the Institute For CyberScience at The Pennsylvania State University for providing computational resources and services that have contributed to the research results reported in this paper. The Institute for Gravitation and the Cosmos is supported by the Eberly College of Science and the Office of the Senior Vice President for Research at the Pennsylvania State University.

References

- Ahmed, S. H., Brooks, A. M., & Christensen, C. R. 2017, *MNRAS*, **466**, 3119
- Allgood, B., Flores, R. A., Primack, J. R., et al. 2006, *MNRAS*, **367**, 1781
- Aubert, D., Pichon, C., & Colombi, S. 2004, *MNRAS*, **352**, 376
- Bahl, H., & Baumgardt, H. 2014, *MNRAS*, **438**, 2916
- Bovy, J. 2015, *ApJS*, **216**, 29
- Buck, T., Dutton, A. A., & Macciò, A. V. 2016, *MNRAS*, **460**, 4348
- Cautun, M., Bose, S., Frenk, C. S., et al. 2015a, *MNRAS*, **452**, 3838
- Cautun, M., Wang, W., Frenk, C. S., & Sawala, T. 2015b, *MNRAS*, **449**, 2576
- Clarke, R. D. 1946, *J. Inst. Actuaries*, **72**, 481
- Conn, A. R., Lewis, G. F., Ibata, R. A., et al. 2013, *ApJ*, **766**, 120
- Helmi, A., White, S. D. M., & Springel, V. 2003, *MNRAS*, **339**, 834
- Henriksen, R. N., & Widrow, L. M. 1997, *PhRvL*, **78**, 3426
- Ibata, N. G., Ibata, R. A., Famaey, B., & Lewis, G. F. 2014, *Natur*, **511**, 563
- Ibata, R. A., Lewis, G. F., Conn, A. R., et al. 2013, *Natur*, **493**, 62
- Johnson, D. R. H., & Soderblom, D. R. 1987, *AJ*, **93**, 864
- Knollmann, S. R., & Knebe, A. 2009, *ApJS*, **182**, 608
- Koposov, S. E., Belokurov, V., Torrealba, G., & Evans, N. W. 2015, *ApJ*, **805**, 130
- Kroupa, P., Theis, C., & Boily, C. M. 2005, *A&A*, **431**, 517
- Libeskind, N. I., Frenk, C. S., Cole, S., et al. 2005, *MNRAS*, **363**, 146
- Libeskind, N. I., Knebe, A., Hoffman, Y., & Gottlöber, S. 2014, *MNRAS*, **443**, 1274
- Lipnicky, A., & Chakrabarti, S. 2017, *MNRAS*, **468**, 1671
- Lovell, M. R., Eke, V. R., Frenk, C. S., & Jenkins, A. 2011, *MNRAS*, **413**, 3013
- Lynden-Bell, D. 1976, *MNRAS*, **174**, 695
- Marinacci, F., Pakmor, R., & Springel, V. 2014, *MNRAS*, **437**, 1750
- McConnachie, A. W. 2012, *AJ*, **144**, 4
- McConnachie, A. W., Irwin, M. J., Ibata, R. A., et al. 2009, *Natur*, **461**, 66
- Metz, M., Kroupa, P., & Libeskind, N. I. 2008, *ApJ*, **680**, 287
- Navarro, J. F., Frenk, C. S., & White, S. D. M. 1996, *ApJ*, **462**, 563
- Papastergis, E., & Shankar, F. 2016, *A&A*, **591**, A58
- Pawlowski, M. S., Famaey, B., Merritt, D., & Kroupa, P. 2015a, *ApJ*, **815**, 19
- Pawlowski, M. S., & Kroupa, P. 2013, *MNRAS*, **435**, 2116
- Pawlowski, M. S., McGaugh, S. S., & Jerjen, H. 2015b, *MNRAS*, **453**, 1047
- Phillips, J. I., Cooper, M. C., Bullock, J. S., & Boylan-Kolchin, M. 2015, *MNRAS*, **453**, 3839
- Sawala, T., Frenk, C. S., Fattahi, A., et al. 2016, *MNRAS*, **457**, 1931
- Smith, R., Flynn, C., Candlish, G. N., Fellhauer, M., & Gibson, B. K. 2015, *MNRAS*, **448**, 2934
- Tempel, E., Stoica, R. S., Martínez, V. J., et al. 2014, *MNRAS*, **438**, 3465
- Zhu, Q., Marinacci, F., Maji, M., et al. 2016, *MNRAS*, **458**, 1559
- Zolotov, A., Brooks, A. M., Willman, B., et al. 2012, *ApJ*, **761**, 71